

MultiNash-PF: A Particle Filtering Approach for Computing Multiple Local Generalized Nash Equilibria in Trajectory Games

Maulik Bhatt¹ Iman Askari² Yue Yu³ Ufuk Topcu⁴ Huazhen Fang² Negar Mehr¹

Abstract—Modern robotic systems frequently engage in complex multi-agent interactions, many of which are inherently multi-modal, meaning they can lead to multiple distinct outcomes. To interact effectively, robots must recognize the possible interaction modes and adapt to the one preferred by other agents. In this work, we propose an efficient algorithm for capturing the multimodality in multi-agent interactions. We leverage a game-theoretic planner to model interaction outcomes as equilibria where *each equilibrium* corresponds to a distinct interaction *mode*. We then develop an efficient algorithm to identify all the equilibria, allowing robots to reason about multiple interaction modes. More specifically, we formulate interactive planning as Constrained Potential Trajectory Games (CPTGs) and model interaction outcomes by local Generalized Nash equilibria (GNEs) of the game. CPTGs are a class of games for which a local GNE can be found by solving a single constrained optimal control problem where a potential function is minimized. We propose to integrate the potential game approach with implicit particle filtering, a sample-efficient method for non-convex trajectory optimization. We utilize implicit particle filtering to identify the coarse estimates of multiple local minimizers of the game’s potential function. MultiNash-PF then refines these estimates with optimization solvers, obtaining different local GNEs. We show through numerical simulations that MultiNash-PF reduces computation time by up to 50% compared to a baseline. We further demonstrate the effectiveness of our algorithm in real-world human-robot interaction scenarios, where it successfully accounts for the multi-modal nature of interactions and resolves potential conflicts in real-time.

I. INTRODUCTION

Modern-world robotics applications are inherently multi-agent in nature. For instance, autonomous cars on highways need to account for other vehicles while planning their motion. Most of the real-world interactions are multi-modal. For example, in the two-player interaction illustrated in Fig. 1, the agents need to move towards their goals while avoiding collisions. Here, two outcomes exist: both agents yielding to their right or left. If the two agents were to act independently, they could reach different outcomes, which would result in a collision. What trajectory each agent would prefer to pick depends on the convention they might be following. For example, in some cultures, in such settings, the convention is to yield to the right to avoid collisions while in other cultures, the convention is to yield to the left. Such conventions

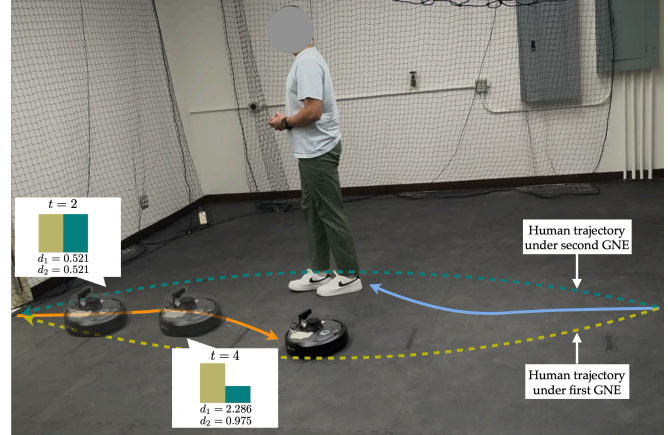


Fig. 1: Snapshot of an interaction between a robot and a human when they exchange positions. Using MultiNash-PF the robot can compute both modes of interaction. At $t = 2$, the robot is uncertain about the preferred mode of the human since the human trajectory’s distance from both equilibria is almost the same. At $t = 4$, the human trajectory is closer to the second GNE therefore, the robot chooses to follow the second GNE accordingly and avoid collision with the human.

usually arise out of recurring coordination problems [1]. Therefore, autonomous agents need to be aware of the existence of multi-modality in the interactions for efficient coordination with people who follow different conventions. Some recent works have shown that computing such multiple trajectories is critical to aligning agents’ preferences over different outcomes [2] or helping coordinate agents’ actions via recommendation [3].

To formalize this problem, we will use dynamic game theory [4] which has shown to be powerful in developing interactive and socially compliant robots [5], [6], [7], [8]. We formulate a multi-agent interactive trajectory planning problem as a *Constrained Potential Trajectory Game* (CPTG). In CPTGs, the interaction outcomes are captured through *generalized Nash equilibrium* (GNE), which are constrained Nash equilibria. When multiple agents- such as robots and humans- interact, a GNE corresponds to a joint action such that no agent has incentives to deviate from its equilibrium actions unilaterally. Several recent works have shown great success in utilizing GNE for multi-agent motion planning in interactive domains [9], [10], [11], [12]. A key challenge in interactive domains, however, is the existence of multiple equilibria, many of which are equally valid. We argue that each equilibrium corresponds to a distinct *mode*

¹Maulik Bhatt and Negar Mehr are with University of California, Berkeley, CA, 94720, USA {maulikbhatt, negar}@berkeley.edu

²Iman Askari and Huazhen Fang are with University of Kansas, Lawrence, KS, 66045, USA {askari, fang}@ku.edu

³Yue Yu is with University of Minnesota, Minneapolis, 55455, USA yuey@umn.edu

⁴Ufuk Topcu is with University of Texas at Austin, TX, 78712, USA utopcu@utexas.edu

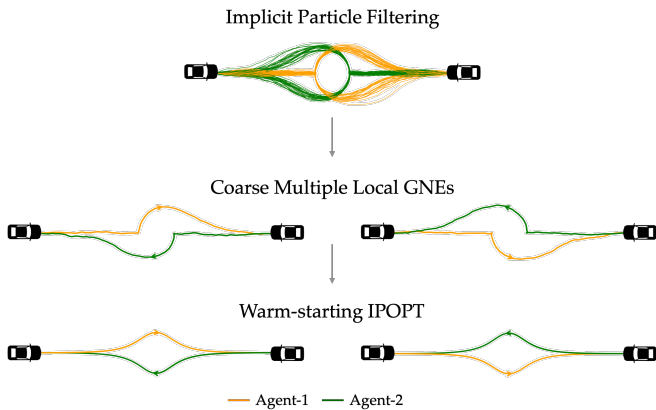


Fig. 2: The Nash equilibrium trajectories found by *MultiNash-PF* when two unicycle agents change their positions. First, we use the implicit particle filter to discover the coarse estimates of two different equilibria, and then utilize them as a warm starting for IPOPT to obtain the two Nash equilibrium trajectories.

of interaction. For instance, in Fig. 1, yielding to the right or left are both acceptable equilibria, representing different Nash equilibria. Consequently, we propose that in order to capture different interaction modes, robots must *reason about multiple interaction equilibria and select the one that aligns with the convention adopted by other agents*.

Computing different local GNEs requires an efficient way to solve games. In practice, computing even a single GNE is often challenging [13] because solving for GNE amounts to solving a set of coupled constrained optimal control problems. Typically, such a solution requires solving first-order KKT conditions of the underlying problems. Therefore, solving the GNE often reduces to addressing a set of complementarity conditions, a process known to be computationally demanding, especially for large-scale applications [14]. Furthermore, computing all the different local GNEs requires initializing the game solvers with many different initial guesses of the equilibrium trajectories from prior knowledge of the specific scenario. This further increases the required number of initial guesses for the game solvers to find all local GNEs. To our best knowledge, there is no principled approach to compute multiple local Nash equilibria in constrained trajectory games other than exhaustive random initializations of the game solvers.

In this paper, we tackle this challenge by introducing *MultiNash-PF*, a novel framework designed to efficiently compute multiple local generalized Nash equilibria (GNEs) in constrained trajectory games. This, in turn, enables robots to recognize and reason about multiple interaction modes. Our approach integrates constrained potential games [15], a class of games that allow for the computation of local GNEs by solving a single constrained optimal control problem, with constraint-aware implicit particle filtering—a sample-efficient method recently applied to nonconvex trajectory optimization [16] to achieve efficient identification of multiple equilibria.

Using CPTGs, we can compute a local GNE by solving a single constrained optimal control problem using off-the-shelf optimization solvers. Then, we use a constraint-aware

implicit particle filtering method to identify multiple local minima of the potential minimization problem. This method eliminates the requirements of random initialization of the optimization solver by efficiently obtaining coarse estimates of different local GNEs. Next, we use the identified minima as initialization for an optimization solver to refine our solution. The solver then computes all the different local GNEs of the original game. Leveraging the sample efficiency of the implicit particle filtering method, *MultiNash-PF* can explore and identify the multiple local GNEs faster than the random initialization of optimization solvers. We further show the real-time application of *MultiNashPF* in a human-robot navigation setting where the robot can reason about the existence of different local GNEs and plan its motion autonomously based on the modality the human prefers.

II. RELATED WORKS

Game Theoretic Planning. One of the earliest works laying the foundation of game theoretic motion planning was [17]. Game theoretic motion planners that seek Stackelberg equilibria were proposed in [18], [7]. Iterative best response methods for computing Nash equilibria were developed in [19], [20]. Iterative linear quadratic approximations to compute Nash equilibria were introduced in [6]. ALGames was developed in [21] which is an augmented lagrangian-based solver for constrained dynamic games. A sequential linear-quadratic technique game-based technique to compute GNE was proposed in [22]. However, these methods are computationally expensive for real-time implementations as the number of agents increases. Potential games-based methods were developed later in [15], [23], [11], [12] to reduce the complexity of computing equilibria. However, the shortcomings of all these methods lie in the fact that they find only one Nash equilibrium of the underlying game and ignore the multi-modal nature of the problem that is crucial for coordination among agents. In [2], the authors recognize the existence of multiple equilibria and focus on inferring the equilibrium of other agents in the environment. However, the methodology relies on computing the different approximate local Nash by rollouts of randomly selected initial strategies, which we show in this work performs poorly compared to our method.

Multiple Local Solutions to Constrained Optimal Control. In general, optimal control problems are often formulated as nonconvex constrained optimization problems, which are solved through the conventional gradient-based approaches such as inter-point methods [24] and sequential quadratic programming [25]. However, given an initialization, they can only find a single local optimal solution. However, in the present context of identifying all potential local GNEs, the gradient-based method would require numerous initializations to find all the local solutions. Departing from gradient-based methods, a Bayesian inference approach has been proposed to solve model predictive control problem [26], [27], [28]. The approach formulates the optimal control problem from a Bayesian inference perspective and employs particle filtering as its estimation method. At

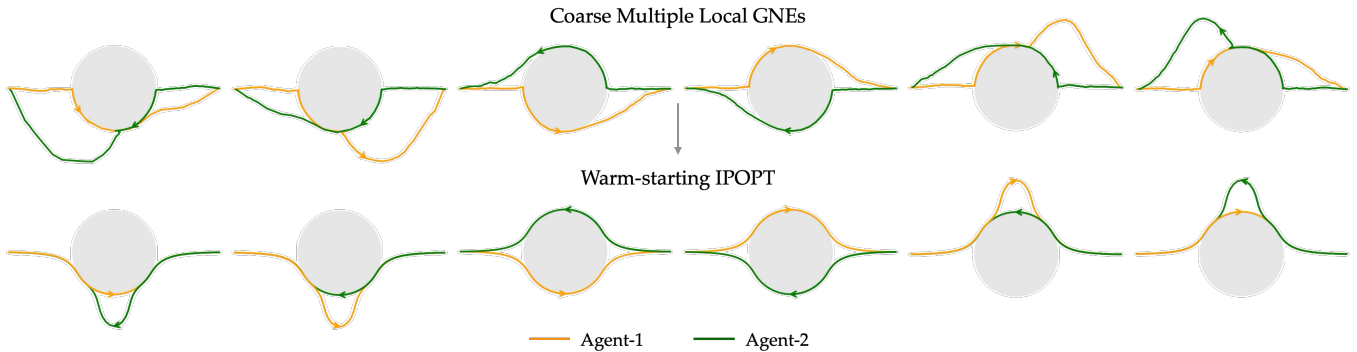


Fig. 3: MultiNash-PF identifies all the local GNE trajectories for a challenging two agent trajectory game where two agents swapped positions while avoiding an obstacle. In this scenario, the obstacle radius is greater than the collision avoidance radius of the two agents, leading to the discovery of 6 distinct Nash equilibria. MultiNash-PF effectively obtains coarse estimates of local GNEs through implicit particle filtering, which are then refined using IPOPT to obtain local GNEs.

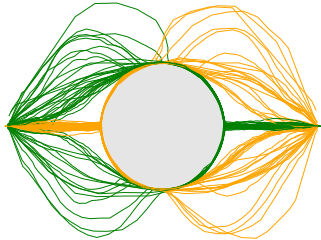


Fig. 4: When using MultiNash-PF on a difficult two agent trajectory game, we first employ an implicit particle filter to obtain coarse estimates of GNEs.

its core, particle filtering utilizes sequential Monte Carlo sampling to perform state estimation for highly nonlinear systems [29], [30]. The efficiency and accuracy of the estimation largely depend on the quality of the sampled particles. Recently, in [31], an efficient particle filtering method was proposed based on the principle of implicit sampling.

III. CONSTRAINED POTENTIAL TRAJECTORY GAMES

We formulate the multi-agent interactive trajectory planning problem as an N -agent constrained potential trajectory game (CPTG). Let $\mathcal{N} := \{1, 2, \dots, N\}$ denote the set of agents' indices. We assume that the game is played over a finite time horizon of $\tau \in \mathbb{N}$ time-steps, where \mathbb{N} is the set of natural numbers.

Let $x_t^i \in \mathbb{R}^{n_i}$ and $u_t^i \in \mathbb{R}^{m_i}$ denote the state and control of the i -th agent at time t , respectively. We assume that the state of the i -th agent evolves as follows:

$$x_{t+1}^i = f^i(x_t^i, u_t^i), \quad (1)$$

for all $t \leq \tau$, where $f^i : \mathbb{R}^{n_i} \times \mathbb{R}^{m_i} \rightarrow \mathbb{R}^{n_i}$ is a continuously differentiable function characterizing the dynamics of the i -th agent. Let $n = \sum_{i=1}^N n_i$, $m = \sum_{i=1}^N m_i$. We denote the joint state, input, and dynamics of all agents as $x_t := [(x_t^1)^\top \ (x_t^2)^\top \ \dots \ (x_t^N)^\top]^\top$, $u_t := [(u_t^1)^\top \ (u_t^2)^\top \ \dots \ (u_t^N)^\top]^\top$, and $f := [(f^1)^\top \ (f^2)^\top \ \dots \ (f^N)^\top]^\top$ respectively. Note that each f^i is a vector-valued dynamics function for each agent. Therefore, $f : \mathbb{R}^n \times \mathbb{R}^m \rightarrow \mathbb{R}^n$ will be a vector-valued dynamics function for the joint system.

In CPTGs, each agent has to satisfy some constraints that couple different agents' states and controls. Let $g : \mathbb{R}^n \times \mathbb{R}^m \rightarrow \mathbb{R}^c$ with $c \in \mathbb{N}$ denote a continuously differentiable function that defines the constraints on the joint state x_t and joint control u_t at each time:

$$g(x_t, u_t) \leq 0_c, \quad (2)$$

where 0_c is a vector of zeros in \mathbb{R}^c . The aim of the constraint function g is to capture individual agents' strict preferences, such as each agent avoiding obstacles, or avoiding collision with other agents. It should be noted that coupling amongst agents' decisions is captured through constraints in CPTGs.

We assume that each agent i aims to minimize an objective function. Let Q^i and Q_τ^i be positive semidefinite and R^i be positive definite matrices for all $i \in \mathcal{N}$. We assume that each agent i seeks to minimize the following objective:

$$\|x_\tau^i - \hat{x}_\tau^i\|_{Q_\tau^i}^2 + \sum_{t=0}^{\tau-1} \|x_t^i - \hat{x}_t^i\|_{Q^i}^2 + \sum_{t=0}^{\tau} \|u_t^i\|_{R^i}^2 \quad (3)$$

where $\hat{x}_t^i \in \mathbb{R}^{n_i}$ is the reference state for agent i at time t . Typically, the reference states for each agent is a path of minimum cost they would follow in the absence of other agents in the environment, e.g., a straight line connecting the start and goal location. Furthermore, we denote the joint reference state of all agents at time t as \hat{x}_t . We use $\text{blkdiag}(A_1, \dots, A_n)$ to denote the block-diagonal of the matrices A_1, \dots, A_n . Let $a_{0:\tau} := \{a_0, \dots, a_\tau\}$ denote the collection of vectors a_t 's over the entire horizon $0 \leq t \leq \tau$. We use $\{x_{0:\tau}^i, u_{0:\tau}^i\}_{i=1}^N$ to denote joint trajectories of all N agents across all times. Note that using the joint notation, we can equivalently write the joint trajectories of all agents as $\{x_{0:\tau}, u_{0:\tau}\}$.

A. Local Generalized Nash Equilibrium Trajectories

Due to the interactive nature of the problem, generally, it is not possible for all agents to minimize their costs simultaneously while satisfying the constraints. Therefore, the interaction outcome is best captured by *local GNE trajectories* of the underlying trajectory game. With dynamics as (1) and constraints as (2), we denote the game by

$$\mathcal{G} := (\mathcal{N}, \{Q^i\}_{i \in \mathcal{N}}, \{Q_\tau^i\}_{i \in \mathcal{N}}, \{R^i\}_{i \in \mathcal{N}}, g, f, \hat{x}_{0:\tau}).$$

For a given ϵ , we define the set of local trajectories around a joint trajectory as $\mathcal{D}(\{x_{0:\tau}, u_{0:\tau}\}, \epsilon) = \left\{ \{x'_{0:\tau}, u'_{0:\tau}\} \mid \sum_{t=0}^{\tau} (\|x_t - x'_t\|_2^2 + \|u_t - u'_t\|_2^2) \leq \epsilon \right\}$. A local GNE trajectory for \mathcal{G} is then defined as follows.

Definition 1. A set of joint trajectories $\{x_{0:\tau}^{i*}, u_{0:\tau}^{i*}\}_{i=1}^N$ is a local GNE trajectory for \mathcal{G} if for all agent $i \in \mathcal{N}$, agent i 's trajectory $\{x_{0:\tau}^{i*}, u_{0:\tau}^{i*}\}$ is an optimal solution of the following optimization problem withing a local neighborhood $\mathcal{D}(\{x_{0:\tau}^*, u_{0:\tau}^*\}, \epsilon)$ for some $\epsilon > 0$:

$$\begin{aligned} \min_{\{x_{0:\tau}^i, u_{0:\tau}^i\}} & \|x_\tau^i - \hat{x}_\tau^i\|_{Q_\tau}^2 + \sum_{t=0}^{\tau-1} \|x_t^i - \hat{x}_t^i\|_{Q_t}^2 + \sum_{t=0}^{\tau} \|u_t^i\|_{R^i}^2 \\ \text{s.t.} & x_0^i = \hat{x}_0^i, x_{t+1}^i = f^i(x_t^i, u_t^i), 0 \leq t \leq \tau - 1, \\ & g(\tilde{x}_t, \tilde{u}_t) \leq 0_c, 0 \leq t \leq \tau, \end{aligned} \quad (4)$$

where we use the following notation in $g(\tilde{x}_t, \tilde{u}_t)$

$$\begin{aligned} \tilde{x}_t &:= [(x_t^{1*})^\top (x_t^{2*})^\top \dots (x_t^{i-1*})^\top (x_t^i)^\top (x_t^{i+1*})^\top \dots (x_t^{N*})^\top]^\top, \\ \tilde{u}_t &:= [(u_t^{1*})^\top (u_t^{2*})^\top \dots (u_t^{i-1*})^\top (u_t^i)^\top (u_t^{i+1*})^\top \dots (u_t^{N*})^\top]^\top. \end{aligned}$$

Intuitively, at a local GNE, no agent can reduce their cost function by independently changing their trajectory to any alternative feasible trajectory within a local neighborhood of the joint equilibrium trajectory, $\{x_{0:\tau}^{i*}, u_{0:\tau}^{i*}\}_{i=1}^N$. Note that in CPTGs, the agents' trajectories are coupled through their joint constraints. It is important to highlight that solving (4) requires solving a set of N coupled constrained optimal control problems, which is often computationally expensive. Therefore, finding all the local GNEs of the game can be time-consuming when using traditional game theoretic methods that aim to solve coupled optimal control problems.

However, an important property of CPTGs is that a GNE of the original game can be computed by optimizing a single constrained optimal control problem called *Potential*, as described in [11]. This reduces the computational cost of computing the GNEs of the game. In the following, we will prove that game \mathcal{G} can be expressed as a constrained trajectory potential game. The following theorem shows that any local minimizer of such a potential function is a local generalized Nash equilibrium trajectory.

Theorem 1. A set of joint trajectories $\{x_{0:\tau}^{i*}, u_{0:\tau}^{i*}\}_{i=1}^N$ is a local GNE trajectory if within a local neighborhood $\mathcal{D}(\{x_{0:\tau}^*, u_{0:\tau}^*\}, \epsilon)$, it is an optimal solution of

$$\begin{aligned} \min_{\{x_{0:\tau}, u_{0:\tau}\}} & \|x_\tau - \hat{x}_\tau\|_{Q_\tau}^2 + \sum_{t=0}^{\tau-1} \|x_t - \hat{x}_t\|_Q^2 + \sum_{t=0}^{\tau} \|u_t\|_R^2 \\ \text{s.t.} & x_0 = \hat{x}_0, x_{t+1} = f(x_t, u_t), 0 \leq t \leq \tau - 1, \\ & g(x_t, u_t) \leq 0_c, 0 \leq t \leq \tau, \end{aligned} \quad (5)$$

for some $\epsilon > 0$, where $Q_\tau := \text{blkdiag}(Q_\tau^1, \dots, Q_\tau^N)$, $Q := \text{blkdiag}(Q^1, \dots, Q^N)$ and $R := \text{blkdiag}(R^1, \dots, R^N)$.

Proof. This theorem follows from [11, Thm. 2]. Since agent costs from (3) depend only on the individual agent's own states and control inputs, we use the results from [11, Thm. 2] to obtain the potential function of \mathcal{G} to be

$$\sum_{i=1}^N \left(\|x_\tau^i - \hat{x}_\tau^i\|_{Q_\tau^i}^2 + \sum_{t=0}^{\tau-1} \|x_t^i - \hat{x}_t^i\|_{Q_t^i}^2 + \sum_{t=0}^{\tau} \|u_t^i\|_{R^i}^2 \right). \quad (6)$$

Furthermore, using the joint notations, we can re-write the sums in (6) as (5). Therefore, we have proven that \mathcal{G} is a CPTG with potential (5). Hence, using Theorem 2 from [11], any local solution of (5) will also be a local GNE of \mathcal{G} . \square

Using Theorem 1, any local solutions of (5) will also be local GNE trajectories. We would like to acknowledge that finding local solutions of (5) will not necessarily give us all the GNEs of the original as Theorem 1 provides only a sufficient condition for computing local GNEs. Furthermore, it is known that the problem of finding all Nash equilibria is a PPAD-complete problem even in the case of static games [13]. However, for all practical purposes in multi-agent navigation, finding local solutions of (5) has proven to be enough for us.

The conventional approach to solving the optimization (5) relies on techniques such as interior point methods [24] or sequential quadratic programming [25]. Naively, the local solutions can be obtained by exhaustive initialization of random trajectories to an optimization solver, such as IPOPT [24], hoping to explore the solution space of local Nash equilibria. However, randomly exploring the nonconvex optimization landscape via gradient-based methods is computationally prohibitive and inefficient, as the same local equilibria can be arrived at from multiple random initializations. To address this, we utilize a Bayesian inference approach in the following section to efficiently recover all local minima of (5).

IV. IDENTIFYING LOCAL NASH EQUILIBRIA VIA BAYESIAN INFERENCE

In this section, we propose our approach to solve (5) from a Bayesian inference perspective. We reformulate the optimal control problem (5) into an equivalent Bayesian inference problem by utilizing the reference trajectory and constraint violations as virtual measurements that provide evidence for the optimal inference of the system trajectory in (5). To this end, we first reformulate problem (5) by considering soft-constraints and introducing auxiliary variables $y_{x,t}$ and $y_{g,t}$ as:

$$\begin{aligned} \min_{\{v_t, w_t, \eta_t\}_{t=0}^{\tau}} & \|v_\tau\|_{Q_\tau}^2 + \sum_{t=0}^{\tau-1} \|v_t\|_Q^2 + \sum_{t=0}^{\tau} \|w_t\|_R^2 + \|\eta_t\|_{Q_\eta}^2, \\ \text{s.t.} & \begin{bmatrix} x_{t+1} \\ u_{t+1} \end{bmatrix} = \begin{bmatrix} f(x_t, u_t) \\ 0_m \end{bmatrix} + \begin{bmatrix} 0_n \\ w_t \end{bmatrix}, \\ & \begin{bmatrix} y_{x,t} \\ y_{g,t} \end{bmatrix} = \begin{bmatrix} x_t \\ \psi(g(x_t, u_t)) \end{bmatrix} + \begin{bmatrix} v_t \\ \eta_t \end{bmatrix}, \\ & \begin{bmatrix} x_0 \\ u_0 \end{bmatrix} = \begin{bmatrix} \hat{x}_0 \\ w_{t-1} \end{bmatrix}, \quad 0 \leq t \leq \tau, \end{aligned} \quad (7)$$

where v_t , w_t , and η_t are bounded disturbances, and $Q_\eta \in \mathbb{R}^{n_c \times n_c}$ assigns the importance of constraint satisfaction. Further, ψ is a barrier function used to quantify the degree of constraint violation by defining

$$\psi(g(x_t, u_t)) = \frac{1}{\alpha} \ln(1 + \exp(g(x_t, u_t))), \quad (8)$$

where α controls the strictness enforcing constraints.

We note that the problem in (7) resembles a moving horizon estimation problem [32]. A direct attempt at solving (7) using traditional gradient-based methods poses a similar computational burden in identifying all of the local equilibria compared to problem (5). However, the above connection between (5) and the moving horizon estimation problem (7) highlights the potential to treat the problem from a Bayesian inference perspective. To this end, we construct the following virtual state-space model from (7) as

$$\bar{x}_{t+1} = \bar{f}(\bar{x}_t) + \bar{w}_t, \bar{y}_t = \bar{h}(\bar{x}_t) + \bar{v}_t, \quad (9)$$

where

$$\bar{x}_t = \begin{bmatrix} x_t \\ u_t \end{bmatrix}, \bar{y}_t = \begin{bmatrix} y_{x,t} \\ y_{g,t} \end{bmatrix}, \bar{w}_t = \begin{bmatrix} 0_n \\ w_t \end{bmatrix},$$

$$\bar{v}_t = \begin{bmatrix} v_t \\ \eta_t \end{bmatrix}, \bar{f}(\bar{x}_t) = \begin{bmatrix} f(x_t, u_t) \\ 0_m \end{bmatrix}, \bar{h}(\bar{x}_t) = \begin{bmatrix} x_t \\ \psi(g(x_t, u_t)) \end{bmatrix},$$

where we relax \bar{w}_t and \bar{v}_t for $0 \leq t \leq \tau$ to be stochastic disturbances modeled as Gaussian-distributed random variables with density

$$\bar{v}_t \sim \mathcal{N}(0_{n+c}, \bar{Q}), \bar{v}_\tau \sim \mathcal{N}(0_{n+c}, \bar{Q}_\tau), \bar{w}_t \sim \mathcal{N}(0_{n+m}, \bar{R}),$$

with $\bar{Q} := \text{blkdiag}(Q^{-1}, Q_\eta^{-1})$, $\bar{Q}_\tau := \text{blkdiag}(Q_\tau^{-1}, Q_\eta^{-1})$, $\bar{R} := \text{blkdiag}(0_{n \times n}, R^{-1})$. The state estimation relevant to (9) is to estimate the state \bar{x}_t given the measurements \bar{y}_t . The value of the virtual measurements must be set in a way that steers the inference problem to have the same optima as in problem (5). We achieve this by noting that $y_{x,t}$ is a measurement value used to correct the state estimate of x_t towards the reference \hat{x}_t . While $y_{g,t}$ is to satisfy constraints through (8). Observing that the barrier function in (8) outputs zero when the constraints are satisfied, we set the virtual measurement for the barrier function equal to 0_c . Hence, the virtual measurement that will drive \bar{x}_t towards optimality takes the value

$$\bar{y}_t = \begin{bmatrix} \hat{x}_t \\ 0_c \end{bmatrix}, 0 \leq t \leq \tau.$$

The Bayesian inference problem pertaining to (9) is one that characterize the conditional distribution $p(\bar{x}_{0:\tau} | \bar{y}_{0:\tau})$. In the following, lemma (1) elucidates that equivalence holds between a posteriori estimate of $p(\bar{x}_{0:\tau} | \bar{y}_{0:\tau})$ and the problem in (5).

Lemma 1. *Assuming independence between the noise vectors \bar{v}_t and \bar{w}_t in (9), the problem in (5) has the same optima as*

$$\bar{x}_{0:\tau}^* = \arg \max_{\bar{x}_{0:\tau}} \log p(\bar{x}_{0:\tau} | \bar{y}_{0:\tau}).$$

We refer the interested reader to [16, Thm. 1] for the proof. The above lemma implies that the local GNEs in (5) translate to multiple local maximums of $p(\bar{x}_{0:\tau} | \bar{y}_{0:\tau})$. Hence, the Bayesian inference problem for (9) involves characterizing the multi-modal PDF $p(\bar{x}_{0:\tau} | \bar{y}_{0:\tau})$. Generally, state estimation of a multi-modal PDF does not admit closed-form solutions [33]. Hence, we resort to approximate solutions. A powerful approach is to use Monte Carlo methods that empirically approximate the distribution via a set of J particles as

$$p(\bar{x}_{0:\tau} | \bar{y}_{0:\tau}) \approx \sum_{j=1}^J w_\tau^j \delta(x_{0:\tau} - x_{0:\tau}^j), \quad (10)$$

where $\delta(\cdot)$ is the dirac delta function and w_τ^j is the weight assigned to a sample trajectory $\bar{x}_{0:\tau}^j$ for $j = 1, \dots, J$.

To achieve the approximation in (10), we employ the implicit particle filter [31] due to the twofold benefit it holds to implement the *MultiNash-PF* framework. First, as suggested in lemma 1, the local maximums (i.e., high-probability regions) of $p(\bar{x}_{0:\tau} | \bar{y}_{0:\tau})$ correspond to the local GNEs. Hence, focusing our sampling efforts towards these high-probability regions can reduce the number of required samples for the approximation in (10). This approach aligns precisely with the principle of implicit importance sampling, whose objective is to build a mapping that draws particles from the high-probability regions of the filtering distribution in (10). Second, we want to avoid the traditionally needed resampling step in particle filtering methods to ensure that the inferred trajectories are smooth. Fortunately, the implicit particle filter does not suffer from the problem of particle degeneracy, and filtering can be achieved by disregarding resampling.

We leverage the Markovian property of the virtual system (9) to recursively approximate (10). Using Bayes' rule, we have

$$p(\bar{x}_{0:t} | \bar{y}_{0:t}) = p(\bar{y}_t | \bar{x}_t) p(\bar{x}_t | \bar{x}_{t-1}) p(\bar{x}_{0:t-1} | \bar{y}_{0:t-1}), \quad (11)$$

for $0 \leq t \leq \tau$. This indicates that given the particle \bar{x}_{t-1}^j from the prior distribution $p(\bar{x}_{0:t-1} | \bar{y}_{0:t-1})$, we can obtain \bar{x}_t^j . As shown in [31], we use implicit importance sampling and identify an implicit mapping to sample from high probability regions of (11). The implicit map is constructed by considering sampling from a reference random vector ξ_t with density $p(\gamma_t)$ and map it to high probability regions of $p(x_{0:t} | y_{0:t})$, such that a sample γ_t^i is mapped to x_t^i . The mapping connects the highly probable regions of $p(\xi)$ to $p(x_{0:t} | y_{0:t})$ by letting

$$F(x_t^i) - \min F(x_t^i) = G(\gamma_t^i) - \min G(\gamma_t^i), \quad (12)$$

where $F(x_t^i) = -\log(p(x_t^i | y_{1:t}))$ and $G(\gamma_t^i) = -\log(p(\gamma_t^i))$. Finding an explicit solution to (12) is computationally intractable due to the involved nonconvex optimization. To bypass this computational challenge, a local Gaussian approximation around \bar{x}_{t-1}^j is employed such that

$$p(\bar{x}_t^j | \bar{y}_{0:t}) \sim \mathcal{N}(\hat{m}_t^j, \hat{\Sigma}_t^{x,j}),$$

where \hat{m}_t^j and $\hat{\Sigma}_t^{x,j}$ are the mean and covariance of \bar{x}_t^j , respectively. These quantities can be approximated recursively using an Unscented Kalman filter (UKF) [34] for all $j = 1, \dots, N$. Then, the implicit map can be computed in closed form as

$$\bar{x}_t^j = \hat{m}_t^j + \sqrt{\hat{\Sigma}_t^{x,j}} \gamma_t^j,$$

where γ_t^j is a sample from $p(\gamma_t) \sim \mathcal{N}(0, I_n)$ and I_n denotes the identity matrix of size n .

This process is repeated until $t = \tau$ for each particle to obtain the set of trajectories $\{\bar{x}_{0:\tau}^j\}_{j=1}^J$, which will include the coarse estimates of local GNEs. This completes

the unscented implicit particle filter, identifying the coarse estimates of multiple local Nash equilibria in (5).

In the last step, the local equilibria are extracted to be from $\{x_{0:\tau}\}_{j=1}^J$. As viewed in Fig. 4, the particle set contains multiple trajectories for each GNE. Therefore, to isolate the GNE trajectories, a clustering method is used to aggregate the particles close to each other in one cluster. One can leverage methods such as hierarchical clustering [35] or DBSCAN [36]. It should be noted that clustering methods require a metric to compute distances between the data points. The Fréchet distance [37] is utilized as our metric to compute distances between the trajectories. The clustering of trajectories will result in one cluster for each GNE by taking the average of trajectories over each cluster and feed them as a warm start to the IPOPT solver to obtain the local GNEs. The algorithmic steps of the proposed *MultiNash-PF* are provided in Algorithm 1.

Algorithm 1 MultiNash-PF: Multiple local GNEs based on particle filter

- 1: Formulate the constrained dynamic potential game (5)
 - 2: Setup the virtual model (9)
Perform unscented implicit particle filtering as follows:
 - 3: Initialize the particles: \bar{x}_0^j , $\hat{\Sigma}_0^{x,j}$, and w_0^j for $j = 1, \dots, J$
 - 4: Employ Algorithm-1 from [31] combined with UKF to obtain coarse solutions, $\{x_{0:\tau}\}_{j=1}^J$.
 - 5: Extract trajectories through clustering from $\{x_{0:\tau}\}_{j=1}^J$ and warm start IPOPT solver to obtain the local GNEs $\{x_{0:\tau}^{i*}, u_{0:\tau}^{i*}\}_{i=1}^N$ of \mathcal{G} .
-

V. NUMERICAL SIMULATIONS

To showcase the capabilities of our method, we take motivation from real-life highway scenarios. We first consider an interaction between two agents moving toward each other as shown in Fig 2. We consider the following discrete-time unicycle dynamics to model each agent $i \in \{1, 2\}$:

$$\begin{aligned} p_{t+1}^i &= p_t^i + \Delta t \cdot v_t^i \cos \theta_t^i, & q_{t+1}^i &= q_t^i + \Delta t \cdot v_t^i \sin \theta_t^i \\ \theta_{t+1}^i &= \theta_t^i + \Delta t \cdot \omega_t^i, & v_{t+1}^i &= v_t^i + \Delta v_t^i, & \omega_{t+1}^i &= \omega_t^i + \Delta \omega_t^i, \end{aligned}$$

where Δt is the time-step size, p_t^i and q_t^i are x and y coordinates of the positions, θ_t^i is the heading angle from positive x -axis, v_t^i is the linear velocity, and ω_t^i is the angular velocity of the agent i at time t . Further, Δv_t^i is the change in linear velocity, and $\Delta \omega_t^i$ is the change in angular velocity of the agent i at time t , respectively. For each agent i , we denote the state vector x_t^i and the action vector u_t^i as follows

$$x_t^i = [p_t^i \quad q_t^i \quad \theta_t^i \quad v_t^i \quad \omega_t^i]^\top, \quad u_t^i = [\Delta v_t^i \quad \Delta \omega_t^i]^\top.$$

We formulate this scenario as a two-player game according to cost functions as described in (3). The reference trajectory for both agents is given as a straight line on the highway, starting from their initial position to their respective goal location. With $\hat{Q} = \text{diag}(50, 10, 5, 5, 2)$, the reference tracking and control effort cost matrices are set as

$$Q^i = 0.6\hat{Q}, \quad Q_\tau^i = 100\hat{Q}, \quad R^i = \text{diag}(8, 4). \quad (13)$$

for $i \in \{1, 2\}$. In addition, the agents are subject to the constraint of avoiding collision with each other, which we define as

$$g_c(x_t, u_t) := -d(x_t^1, x_t^2) + r_{\text{col}} \leq 0, \quad (14)$$

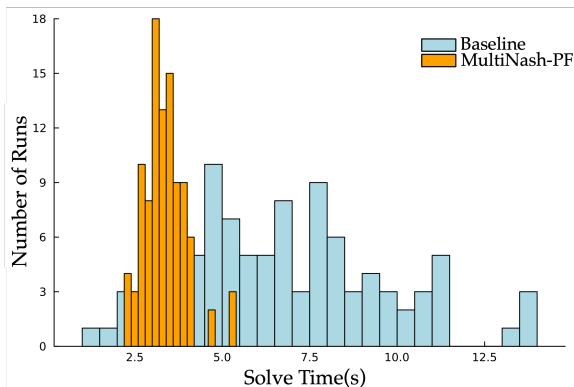
where $d(x_t^1, x_t^2) := \sqrt{(p_t^1 - p_t^2)^2 + (q_t^1 - q_t^2)^2}$ is the Euclidean distance between the two agents and $r_{\text{col}} := 3m$ is the collision avoidance radius between the two agents.

With this setup, we employ MultiNash-PF from Algorithm 1 to efficiently capture the multi-modality in the solution space and then extract the solutions using hierarchical clustering [35] to provide a warm start trajectory to IPOPT [24] solver to recover different local GNEs. We use the Julia programming language and utilize the JuMP [38] library to solve the game using the IPOPT solver. The results of our method are provided in Fig 2. As we can see, the presence of two agents and collision avoidance constraints induces two different possible GNEs. Either both the agents will yield to their right, or they will yield to their left to avoid collision. As shown in Fig 2, our method can recover both equilibria.

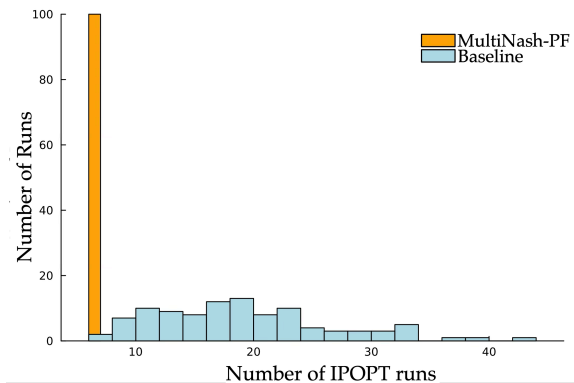
Furthermore, we consider a more complicated scenario in which two agents aim to exchange their positions while avoiding an obstacle of radius $r_{\text{obs}} = 4m$ located at the midpoint of the two agents. It should be noted that the radius of the obstacle is larger than the collision avoidance radius of the two agents.

We consider the same unicycle dynamics as before, and the reference trajectory cost is also the same as in (13). Furthermore, the collision avoidance radius between the two agents is also the same as before. In addition to (14), the constraints for this game will include both agents avoiding the obstacle $g_o^i(x_t, u_t) := [-d(x_t^i, x_{\text{obs}}) + r_{\text{obs}}]$ for $i = 1, 2$ where x_{obs} is the location of the obstacle. We also assume that we have constraints on the control bounds $g_b(x_t, u_t) = [-v_t^1, -v_t^2, |u_t^1| - u_b^1, |u_t^2| - u_b^2]$, where u_b^1 and u_b^2 are controlled action bounds for agents 1 and 2, respectively. We write the combined constraints as $g(x_t, u_t) := [g_c \quad g_o^1 \quad g_o^2 \quad g_b]^\top \leq 0$. We choose the values of control action bounds to be $u_b^1 = u_b^2 = [0.15, 0.75]^\top$. This setup induces multitudes of local equilibria. Two trivial local equilibria are when the two agents pass each other through opposite sides of the obstacle. However, there exist four other nontrivial equilibria when both agents can go on the same side of the obstacle, and one of the agents can yield to the other one. It is challenging to recover all six equilibria without utilizing the capabilities of the implicit particle filter. Upon performing simulation experiments with our method, we observe that MultiNash-PF can recover all six Nash equilibria as shown in Fig. 4 and Fig. 3.

1) *Comparison with Baseline*: In order to compare the effectiveness of our method, we consider a baseline method. In the baseline method, we directly initialize the IPOPT solver with random perturbations of reference trajectories and compute the resulting optimal solutions. For our method, we fixed $J = 50$ particles and obtained the solution trajectories using implicit particle filtering from Algorithm 1



(a) Histogram of the solve time comparison of MultiNash-PF and the baseline.



(b) Histogram of the number of the IPOPT runs required to obtain all six equilibria.

Fig. 5: Comparison of MultiNash-PF with the baseline for the experiment shown in Fig. 3.

(a) The average solve time for MultiNash-PF is $3.36 \pm 0.59s$ while the baseline’s average solve time is $6.71 \pm 2.83s$. MultiNash-PF reduces the solve time by about 50% compared to the baseline while giving a much lower variance on the solve time. (b) For the baseline, the average number of IPOPT runs required to obtain all six different equilibria is 18.64 ± 7.57 , while for MultiNash-PF, this is always 6. MultiNash-PF requires 3 times fewer IPOPT runs.

described in Section IV. After that, we extract all the different equilibria and provide them as a warm starting point for IPOPT to obtain the final solutions. The compute time of our method is a combination of time used in implicit particle filtering and time used by IPOPT to obtain all the different equilibria given warm starting from filtering.

We run the IPOPT solver until we recover all 6 different equilibria. We repeat this experiment for 100 different Monte Carlo runs. We observe that it requires, on average, 18.64 ± 7.57 number of IPOPT runs to obtain all six different equilibria using the baseline approach of random warm-starting. However, with our method, the number of IPOPT runs required is always six because we always obtain all six modes of equilibria from implicit particle filtering. A histogram of the number of IPOPT runs required for obtaining all six equilibria is plotted in Fig. 5b.

Furthermore, the solve time to recover all 6 different Nash equilibria for the baseline is $6.71 \pm 2.83s$, while for MultiNash-PF, the solve time is $3.36 \pm 0.59s$. Our method results in a solve-time reduction of 50% compared

to the baseline while giving a much lower variance on the solve time. A histogram of the solve times of the baseline compared to our method is plotted in Fig. 5a. As explained earlier, our method’s solve time is a combination of the time used in implicit particle filtering and the time used by IPOPT. We observe that the time required for implicit particle filtering over 100 Monte Carlo runs is $0.37 \pm 0.072s$ while the time used by IPOPT to obtain the final solutions is $2.99 \pm 0.57s$. Therefore, in our MultiNash-PF, the time used by implicit particle filtering is 11% of the total solve time, which shows that filtering is very efficient in exploring the solution space of local Nash equilibria and contributes really less to the overall computation time of MultiNash-PF.

VI. HARDWARE EXPERIMENT

Finally, we conduct a hardware experiment where a human and a robot exchange their position as shown in Fig. 1. We perform these experiments using a TurtleBot 4 which is a ground robot with unicycle dynamics. We assume that the human also follows unicycle dynamics. The collision avoidance constraint between the TurtleBot and human is assumed to be the same as of (14). We use the Vicon motion capture system to measure the current position of both the robot and the human.

Similar as shown in Fig. 2, two GNEs may exist which will correspond to two different modes of interactions. Namely, either the human and robot yield to their right or they yield to their left. For the robot to safely navigate around the human without collision, the robot needs to be aware of both the GNEs and needs to be able to determine which GNE the human chooses. Using MultiNashPF, the robot first uses an implicit particle filter to obtain the coarse estimates of the two different equilibria and then utilizes them as a warm start for IPOPT to obtain two modes of interaction. We assume that the interaction happens over $T = 10s$. Then similar to [11], the robot uses a potential function based game theoretic planner in a model-predictive fashion with a planning horizon of 5s and $\Delta t = 0.1s$ to plan its motion.

The robot faces two choices of GNEs to follow recovered from the MultiNashPF. At any given time t of planning, the robot computes the Fréchet distance [37] between the trajectory exhibited by the human so far and the human’s trajectory in both the computed GNEs. Let the distances of human trajectory from both the GNEs be denoted by d_1 and d_2 , respectively. The robot keeps an uncertainty on the GNE that the human chooses until $|d_1 - d_2| > d^*$ where d^* is the specified threshold. For example, in Fig. 1 at $t = 2$, values of d_1 and d_2 are almost identical which indicates that human has not chosen their mode of interaction. Whenever $|d_1 - d_2| > d^*$ occurs, the robot becomes certain of the mode of interaction followed by the human. Then the robot follows GNE corresponding to $\arg \min_{i \in \{1,2\}} \{d_i\}$. For example, in Fig. 1, at $t = 4$, the Fréchet distance of the human from its first GNE trajectory is very high while for the second GNE, the Fréchet distance is low indicating that the human has chosen the second GNE which corresponds to both the agents yielding to their right. Using our method, the robot

autonomously identifies this mode, moves accordingly, and reaches its goal location while successfully avoiding collision with the human.

We ran 10 different trials and each time we asked the human to either yield to their right or left randomly. Our algorithm was able to successfully compute both modes and identify the mode that the human was following. Using our algorithm, the robot was able to successfully avoid collision with the human in real-time and reach its goal location in all 10 runs.

VII. CONCLUSION

In this work, we introduced MultiNash-PF, a novel algorithm for efficiently computing multiple local GNEs in CPTGs. By leveraging potential game theory and implicit particle filtering, MultiNash-PF efficiently identifies coarse estimates of local minimizers, which are then refined using optimization solvers to obtain distinct interaction modes. Our numerical simulations demonstrate that MultiNash-PF significantly reduces computation time—by up to 50% compared to baseline methods—while effectively capturing the multimodal nature of multi-agent interactions. Furthermore, our real-world human-robot interaction experiments highlight the algorithm’s ability to reason about multiple interaction modes and resolve conflicts in real-time. These results underscore the potential of MultiNash-PF to enhance interactive motion planning, enabling more adaptive and socially aware autonomous systems.

REFERENCES

- [1] R. Alterman and A. Garland, “Convention in joint activity,” *Cognitive Science*, vol. 25, no. 4, pp. 611–657, 2001.
- [2] L. Peters, D. Fridovich-Keil, C. J. Tomlin, and Z. N. Sunberg, “Inference-based strategy alignment for general-sum differential games,” *arXiv preprint arXiv:2002.04354[cs.RO]*, 2020.
- [3] J. Im, Y. Yu, D. Fridovich-Keil, and U. Topcu, “Coordination in noncooperative multiplayer matrix games via reduced rank correlated equilibria,” *arXiv preprint arXiv:2403.10384[cs.GT]*, 2024.
- [4] T. Başar and G. J. Olsder, *Dynamic noncooperative game theory*. SIAM, 1998.
- [5] G. Galati, S. Primatesta, S. Grammatico, S. Macrì, and A. Rizzo, “Game theoretical trajectory planning enhances social acceptability of robots by humans,” *Scientific Reports*, vol. 12, no. 1, p. 21976, 2022.
- [6] D. Fridovich-Keil, E. Ratner, L. Peters, A. D. Dragan, and C. J. Tomlin, “Efficient iterative linear-quadratic approximations for nonlinear multi-player general-sum differential games,” in *2020 IEEE International Conference on Robotics and Automation (ICRA)*, pp. 1475–1481, IEEE, 2020.
- [7] D. Sadigh, S. Sastry, S. A. Seshia, and A. D. Dragan, “Planning for autonomous cars that leverage effects on human actions,” in *Robotics: Science and systems*, vol. 2, pp. 1–9, Ann Arbor, MI, USA, 2016.
- [8] M. Bhatt and N. Mehr, “Strategic decision-making in multi-agent domains: A weighted potential dynamic game approach,” *arXiv preprint arXiv:2308.05876*, 2023.
- [9] A. Dreves and M. Gerdts, “A generalized Nash equilibrium approach for optimal control problems of autonomous cars,” *Optimal Control Applications and Methods*, vol. 39, no. 1, pp. 326–342, 2018.
- [10] M. Wang, N. Mehr, A. Gaidon, and M. Schwager, “Game-theoretic planning for risk-aware interactive agents,” in *2020 IEEE/RSJ International Conference on Intelligent Robots and Systems (IROS)*, pp. 6998–7005, IEEE, 2020.
- [11] M. Bhatt, Y. Jia, and N. Mehr, “Efficient constrained multi-agent trajectory optimization using dynamic potential games,” in *2023 IEEE/RSJ International Conference on Intelligent Robots and Systems (IROS)*, pp. 7303–7310, IEEE, 2023.
- [12] Y. Jia, M. Bhatt, and N. Mehr, “Rapid: Autonomous multi-agent racing using constrained potential dynamic games,” in *2023 European Control Conference (ECC)*, pp. 1–8, IEEE, 2023.
- [13] C. Daskalakis, P. W. Goldberg, and C. H. Papadimitriou, “The complexity of computing a Nash equilibrium,” *Communications of the ACM*, vol. 52, no. 2, pp. 89–97, 2009.
- [14] F. Facchinei and C. Kanzow, “Generalized Nash equilibrium problems,” *Annals of Operations Research*, vol. 175, no. 1, pp. 177–211, 2010.
- [15] S. Zazo, S. V. Macua, M. Sánchez-Fernández, and J. Zazo, “Dynamic potential games with constraints: Fundamentals and applications in communications,” *IEEE Transactions on Signal Processing*, vol. 64, no. 14, pp. 3806–3821, 2016.
- [16] I. Askari, X. Tu, S. Zeng, and H. Fang, “Model predictive inferential control of neural state-space models for autonomous vehicle motion planning,” *arXiv preprint arXiv:2310.08045*, 2023.
- [17] S. M. LaValle, “Robot motion planning: A game-theoretic foundation,” *Algorithmica*, vol. 26, pp. 430–465, 2000.
- [18] A. Liniger and J. Lygeros, “A noncooperative game approach to autonomous racing,” *IEEE Transactions on Control Systems Technology*, vol. 28, no. 3, pp. 884–897, 2019.
- [19] R. Spica, E. Cristofalo, Z. Wang, E. Montijano, and M. Schwager, “A real-time game theoretic planner for autonomous two-player drone racing,” *IEEE Transactions on Robotics*, vol. 36, no. 5, pp. 1389–1403, 2020.
- [20] M. Wang, Z. Wang, J. Talbot, J. C. Gerdes, and M. Schwager, “Game theoretic planning for self-driving cars in competitive scenarios,” in *Robotics: Science and Systems*, 2019.
- [21] S. Le Cleac’h, M. Schwager, and Z. Manchester, “Algames: a fast augmented lagrangian solver for constrained dynamic games,” *Autonomous Robots*, vol. 46, no. 1, pp. 201–215, 2022.
- [22] F. Laine, D. Fridovich-Keil, C.-Y. Chiu, and C. Tomlin, “The computation of approximate generalized feedback Nash equilibria,” *SIAM Journal on Optimization*, vol. 33, no. 1, pp. 294–318, 2023.
- [23] T. Kavuncu, A. Yaraneri, and N. Mehr, “Potential iLQR: A potential-minimizing controller for planning multi-agent interactive trajectories,” *arXiv preprint arXiv:2107.04926*, 2021.
- [24] A. Wächter and L. T. Biegler, “On the implementation of an interior-point filter line-search algorithm for large-scale nonlinear programming,” *Mathematical Programming*, vol. 106, no. 1, pp. 25–57, 2006.
- [25] P. T. Boggs and J. W. Tolle, “Sequential quadratic programming,” *Acta numerica*, vol. 4, pp. 1–51, 1995.
- [26] D. Stahl and J. Hauth, “PF-mpc: Particle filter-model predictive control,” *Systems & Control Letters*, vol. 60, no. 8, pp. 632–643, 2011.
- [27] I. Askari, S. Zeng, and H. Fang, “Nonlinear model predictive control based on constraint-aware particle filtering/smoothing,” in *2021 American Control Conference (ACC)*, pp. 3532–3537, IEEE, 2021.
- [28] I. Askari, B. Badnava, T. Woodruff, S. Zeng, and H. Fang, “Sampling-based nonlinear MPC of neural network dynamics with application to autonomous vehicle motion planning,” in *2022 American Control Conference (ACC)*, pp. 2084–2090, IEEE, 2022.
- [29] A. Doucet, N. De Freitas, N. J. Gordon, *et al.*, *Sequential Monte Carlo methods in practice*, vol. 1. Springer, 2001.
- [30] S. Särkkä and L. Svensson, *Bayesian filtering and smoothing*, vol. 17. Cambridge university press, 2023.
- [31] I. Askari, M. A. Haile, X. Tu, and H. Fang, “Implicit particle filtering via a bank of nonlinear Kalman filters,” *Automatica*, vol. 145, p. 110469, 2022.
- [32] C. Rao, J. Rawlings, and D. Mayne, “Constrained state estimation for nonlinear discrete-time systems: stability and moving horizon approximations,” *IEEE Transactions on Automatic Control*, vol. 48, no. 2, pp. 246–258, 2003.
- [33] S. Särkkä, *Bayesian Filtering and Smoothing*. Institute of Mathematical Statistics Textbooks, 2013.
- [34] E. A. Wan and R. Van Der Merwe, “The unscented kalman filter for nonlinear estimation,” in *Proceedings of the IEEE 2000 adaptive systems for signal processing, communications, and control symposium (Cat. No. 00EX373)*, pp. 153–158, Ieee, 2000.
- [35] F. Murtagh and P. Contreras, “Algorithms for hierarchical clustering: an overview,” *Wiley Interdisciplinary Reviews: Data Mining and Knowledge Discovery*, vol. 2, no. 1, pp. 86–97, 2012.
- [36] M. Ester, H.-P. Kriegel, J. Sander, X. Xu, *et al.*, “A density-based algorithm for discovering clusters in large spatial databases with noise,” in *kdd*, vol. 96, pp. 226–231, 1996.
- [37] T. Eiter and H. Mannila, “Computing discrete fréchet distance,” 1994.
- [38] I. Dunning, J. Huchette, and M. Lubin, “Jump: A modeling language for mathematical optimization,” *SIAM review*, vol. 59, no. 2, pp. 295–320, 2017.